Journal of Instrumentation

readPTU: a python library to analyse time tagged time resolved data

Published by IOP Publishing for Sissa Medialab

Received: *March 13, 2019*
Accepted: *May 17, 2019*
Published: *June 27, 2019*

TECHNICAL REPORT

readPTU: a python library to analyse time tagged time resolved data

G.C. Ballesteros,[1] **R. Proux, C. Bonato and B.D. Gerardot**

Institute of Photonics and Quantum Sciences (IPaQS), Heriot-Watt University, Edinburgh, EH14 4AS, U.K.

E-mail: gb173@hw.ac.uk

Abstract: readPTU is a python package designed to analyze time-correlated single-photon counting data. The use of the library promotes the storage of the complete time arrival information of the photons and full flexibility in post-processing data for analysis. The library supports the computation of time resolved signal with external triggers and second order autocorrelation function analysis can be performed using multiple algorithms that provide the user with different trade-offs with regards to speed and accuracy. Additionally, a thresholding algorithm to perform time post-selection is also available. The library has been designed with performance and extensibility in mind to allow future users to implement support for additional file extensions and algorithms without having to deal with low level details. We demonstrate the performance of readPTU by analyzing the second-order autocorrelation function of the resonance fluorescence from a single quantum dot in a two-dimensional semiconductor.

Keywords: Analysis and statistical methods; Data processing methods

[1]Corresponding author.

https://doi.org/10.1088/1748-0221/14/06/T06011

2019 JINST 14 T06011

Contents

1 Motivation and significance **1**

2 Autocorrelation measurements using TCSPC **2**
2.1 From photon statistics to $g^{(2)}(\tau)$ 2
2.2 Algorithms 3
2.3 Intensity time trace 3
2.4 $g^{(2)}(t)$ algorithms 3
2.4.1 Naive algorithm 3
2.4.2 Ring algorithm 4
2.5 readPTU 5
2.5.1 Sample usage 7

3 Example: resonance fluorescence of a quantum emitter with spectral fluctuations **7**

4 Conclusions **10**

1 Motivation and significance

Time-correlated single-photon counting (TCSPC) experiments have found widespread applications in different disciplines, including the characterization of individual optical emitters [1, 2], advanced microscopy [3, 4], Bell's inequalities verification using astronomical sources [5], or the real time tracking of physiochemical reactions [6]. This technique is also a major tool for the characterization of single photon emission [2, 7, 8], relevant for quantum technologies such as linear optics quantum computing [9] and spin-photon interfaces for quantum communication networks [10, 11]. TCSPC measurements can be used to characterize the statistical properties of the emitted light [12] and it is thus a tool to prove the single-photon nature of a source and provide useful information about its internal dynamics.

When recording TCSPC data, one usually only directly computes the quantities of interest, such as a histogram of the delays between photon clicks at two channels, since storing the timing information for all detector clicks can easily grow above gigabyte sizes. On the other hand, storing this information can be advantageous to perform more sophisticated data analysis. For example, time traces of the detected detector click rates can reveal intensity spikes and the emitters' dynamics, or enable post selection of specific time intervals. The readPTU[1] library presented here enables the researcher to achieve this, providing added flexibility in their experiments.

The library has been written as a Python module that interfaces with a C library that handles the most computing-intensive aspects. This combination provides a user-friendly interface to a high performance set of underlying routines. The underlying C library provides functionalities to efficiently

[1]The repository for the readPTU is hosted at: https://github.com/qpl-public/readPTU.

2019 JINST 14 T06011

read a stream of detector click records, with no required knowledge about the low level details of how the information is encoded on the binary files, making the library of algorithms easy to extend. Several other software packages with similar functionality have been published [13, 14]. We believe readPTU represents a significant improvement due to its focus on providing a user-friendly interface to a highly performant library and the addition of new algorithms to perform time post-selection.

Our hope is that the work presented here will allow researchers across a variety of disciplines to analyze raw TCSPC data more efficiently.

2 Autocorrelation measurements using TCSPC

One of the main applications of TCSPC is the characterization of the statistical properties of a light source, such as the anti-bunched nature of single photon sources, through the second order autocorrelation of the field. The right panel of figure 1 shows a simplified setup of such an experiment. The emitted photon field is split by a 50/50 beam splitter and directed to two single photon detectors, such as avalanche photo diodes (APS) or super conducting nanowire single photon detectors (SNSPD). Upon photon detection, detector clicks are recorded by channels A and B of time-Correlated single photon counting system (TCSPC). Since a single photon source cannot produce a click on both channels simultaneously, a dip is observed in the coincidence rate when the delay between the channels is equal (figure 1, left panel). This result is only possible under the assumption that the electromagnetic field is quantized [12]. These results can be extended to the n-th order correlation functions and provide a full characterization of the coherence properties of an electromagnetic field.

In this section we will introduce the basic theory behind the second order autocorrelation function and how it can be experimentally measured using TCSPC. To compute the second order autocorrelation function, $g^{(2)}(\tau)$, we need to consider first what is the probability amplitude for measuring a photon with a delay of Δt in detector B after a having measured one in detector A. This is given by [15]:

$$\langle f|E_A^{(+)}(t)E_B^{(+)}(t+\Delta t)|i\rangle \tag{2.1}$$

where $E^{(+)}(r,t)$ is the photon annihilation operator and $|i\rangle$ and $|f\rangle$ are the initial and final states respectively. Similarly we can define the probability of detecting two photons in different detectors ($r = A, B$). We will show in section 2.1 how considering all final states and averaging over the ensemble of initial states leads to the definition of the second order autocorrelation function $G^{(2)}(\tau)$:

$$G^{(2)}(\tau) = \langle E^{(-)}(0)E^{(-)}(\tau)E^{(+)}(\tau)E^{(+)}(0)\rangle \tag{2.2}$$

In the latter expressions we have fixed $t = 0$ under the assumption that we are dealing with a stationary process, in that the value of the autocorrelation function will only depend on time differences.

2.1 From photon statistics to $g^{(2)}(\tau)$

We show now how building a histogram of time delays between photons in channel A and channel B of the TCSPC system gives us access to the second order autocorrelation function of a stream of photons. Put another way, this histogram gives an approximation to the joint probability distribution of measuring a photon in the first detector in between times $t + \mathrm{d}t$ and $t + \tau + \mathrm{d}t$ on the second

2019 JINST 14 T06011

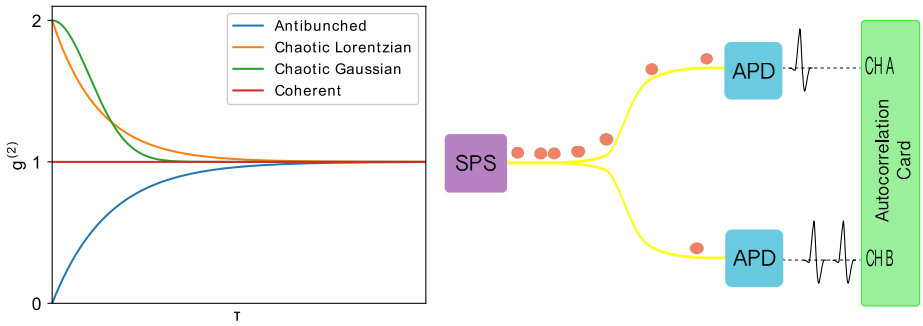

Figure 1. (Left) Typical second order autocorrelation functions for different types of sources. Only anti-bunched light will show a dip going to zero at $\tau = 0$ indicating that two photons never arrived simulatenausly at both channels. (Right) Experimental setup to measure the second order autocorrelation from a single photon source.

detector [16]. The probability per unit time to obtain the final state $|f\rangle$ after the detection of a photon at t in channel A and at $t + \tau$ in channel B from the initial state $|i\rangle$ is proportional to:

$$w_{2,if}(\tau) = |\langle f|E^{(+)}(\tau)E^{(+)}(0)|i\rangle|^2 \tag{2.3}$$

If we sum over all possible final states and introduce the density operator ($\rho = \sum_{i'} P_{i'}|i'\rangle\langle i'|$) to consider the mixture of initial states we conclude that:

$$w_2(\tau) = Tr[\rho E^{(-)}(0)E^{(-)}(\tau)E^{(+)}(\tau)E^{(+)}(0)] = G^{(2)}(\tau) \tag{2.4}$$

2.2 Algorithms

readPTU provides multiple algorithms to postprocess TCSPC data, each featuring different trade-offs.

2.3 Intensity time trace

The first algorithm provided by readPTU enables user to obtain a time-trace of the photon count. Its pseudo-code is shown in Algorithm 1. The algorithm goes through the recorded photon events and assigns them to the current time bin as long as its time-tag falls within it. Once the time tag is larger than the end time of the current time bin, CurrBin is updated and the next time bin starts to be filled. The length of each time bin sets the trade-off between time resolution and the error in the photon count due to Poissonian statistics. The intensity time-trace can be used to study emitter dynamics as will be demonstrated in section 3.

2.4 $g^{(2)}(t)$ algorithms

2.4.1 Naive algorithm

The derivation in section 2.1 shows how $g^{(2)}(\tau)$ can be approximated by a histogram of the delays between photon clicks in channels A and B of the autocorrelation card. The simplest implementation of this idea is described in figure 2 and Algorithm 2.

When a photon is detected in channel A, a stopwatch is started. When, after a time delay dt a second photon is recorded at channel B, dt is assigned to the histogram in the call to *UpdateHistogram*

2019 JINST 14 T06011

Algorithm 1 Timetrace algorithm.

```
procedure TimeTrace
    EndOfBin ← dT
    n ← 0
    CurrBin ← 0
    while n < NumRecrods do
        (channel, t) ← ParseNextRecord
        if t < EndOfBin then
            n ← n + 1
        else if t > EndOfBin then
            UpdateTimeTrace(n, CurrBin)
            EndOfBin ← EndOfBin + dT
            n ← 1
            CurrBin ← CurrBin + 1
        end if
    end while
end procedure
```

and the process repeated. The *UpdateHistogram* function additionally checks if the measured delay is within a user defined interval (the autocorrelation window) that establishes the longest delay that will be stored in the output histogram.

An artificial delay between the two channels is typically added to shift $t = 0$ from the origin, so that $g^{(2)}(t = 0)$ can be see when running the autocorrelator in histogram mode. Reversing start and stop channels brings the $t = 0$ autocorrelation out of the histogram: readPTU library has an operation mode that removes this issue by running an algorithm symmetric on the assignment of start and stop channels. Although this algorithm is extremely fast and good enough for quickly exploring the data it has two major shortcomings. First, the time delay between two consecutive photons follows an exponential distribution. Since the algorithm described above only looks at consecutive pairs, an exponential decay artifact is introduced. Second, photons in channel A are ignored while waiting for a click in channel B, wasting available information (see the photons greyed out in figure 2).

2.4.2 Ring algorithm

The ring algorithm presented here (pseudo-code in Algorithm 3) fixes both shortcomings highlighted in the previous section in a numerically efficient way. Click times for channel A are stored in a buffer. Whenever detector B clicks, the algorithm loops over the click times stored in the buffer and generates a list of time delays, which are then stored in the histogram. Each time a photon clikcs at channel A, if the buffer is full, the oldest photon click is replaced for the newly detected, hence the ring (buffer) name. Even though this greatly mitigates the exponential artifacts shown by the naive algorithm, a situation may occur where a time delay is larger than the correlation window. This situation is corrected by keeping track of the longest seen delay on a loop over the start photon buffer. If a delay bigger than the correlation window is encountered the buffer is doubled in size.

Algorithm 2 Naive algorithm.

```
procedure NAIVE
    WaitForStop ← FALSE
    n ← 0
    while n < NumRecrods do
        (channel, t) ← ParseNextRecord
        n ← n + 1
        if channel == start AND NOT WaitForStop then
            StartTime ← t
            WaitForStop ← TRUE
        else if channel == stop AND WaitForStop then
            dt ← t − StartTime
            UpdateHistogram(dt)
            WaitForStop ← FALSE
        end if
    end while
end procedure
```

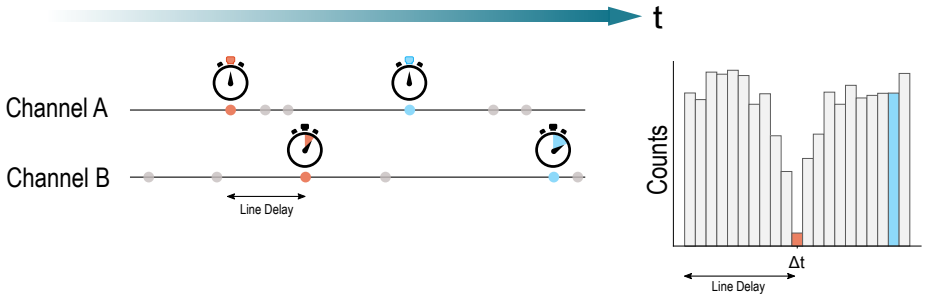

Figure 2. Schematic representation of the naive algorithm. When the first (red) photon arrives at channel A, a stopwatch is started. When a photon arrives at channel B, the stopwatch is stopped and the delta introduced in a histogram. After the stop photon in channel B has arrived we wait for another photon to arrive at channel A and repeat the process. Notice how all the greyed out photons haven't been used to compute the autocorrelation function. This leads to a less efficient use of the data available and an exponential decaying artifact on the computed solution.

2.5 readPTU

readPTU is distributed as a Python library with a compiled C component, running under Windows, MacOS and Linux. Its main goal is to provide a user-friendly interface via Python to users wanting to postprocess multi-gigabyte files of TCSPC data. It currently supports calculation of intensity time traces and $g^{(2)}$ autocorrelations (with/without post-selection).

The main C file acts as a template for (currently) 3 dynamically linked libraries. Each of the libraries provides support for a different input file format. Currently T2 mode files for the HydrapHarp, TimeHarp, PicoHarp and HydraHarp2 devices from PicoQuant are supported. Instructions on how to add new files formats is explained in the package documentation. Each file format requires a

Algorithm 3 Ring algorithm.

```
procedure RING
    WaitForStop ← FALSE
    n ← 0
    while n < NumRecrods do
        (channel, t) ← ParseNextRecord
        n ← n + 1
        if channel == start then
            StorePhoton(t)
        else if channel == stop then
            for t_start in PhotonBuffer do
                dt ← t − t_start
                UpdateHistogram(dt)
            end for
        end if
    end while
end procedure
```

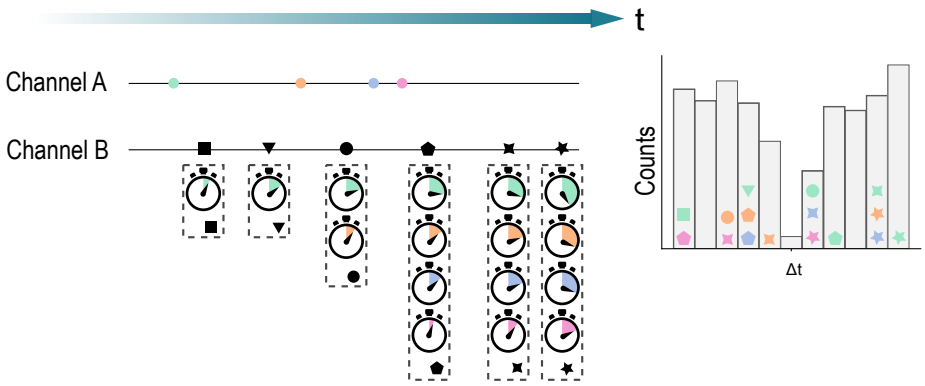

Figure 3. Schematic representation of the ring algorithm. By introducing a buffer for the start channel (A) we can compute delays with respect to all the photons arriving at channel B. Every time a photon is detected on channel B a set of delays with respect to all the photons in channel's A buffer is computed. The computed delays are represented in the boxes below each photon in Channel B. With the naive algorithm it would not have been possible to use the triangle photon (ch B) as we would have been waiting idly to detect a photon on channel A. It also would not have been possible to use the pink photon (ch A) as we would have been waiting for a stop photon in channel B.

2019 JINST 14 T06011

parser to be defined in *parsers.c*. Through using different libraries, the overhead from dynamically selecting (via function pointers or switch statements) what specific file format parser to use is completely removed, while keeping a single codebase and an easily extensible system for future file formats. The whole library has been designed to primarily target performance: to this end, buffered input and output is used by reading multiple records from the TCSPC files simultaneously. This optimization reduces by three orders of magnitude the number of file read operations required to process the input. Memory locality was taken into account by substituting the use of linked lists for contiguous memory arrays. Additionally, all the functions provided by the library offer multithread support to take advantage of modern multi-core CPUs. The parallelization strategy is based on analyzing different ranges of records in the TCSPC files separately and the combining the results together. This means that there are no shared variables among the different threads and the algorithms don't require the use of synchronization primitives. Detector click times are time-ordered in the buffers used by Algorithm 3; this allows one to introduce a check to break out of the histogram updating loop as soon as a time delay longer than the one that can fit in the histogram is detected.

2.5.1 Sample usage

readPTU is designed to be as user-friendly as possible. The code listing below presents an example of how to use the library to obtain a timetrace and compute the $g^{(2)}(\tau)$ from TCSPC data.

Files are opened within **With** block to make sure that the file is appropriately closed when no longer needed. The *timetrace* function has only one mandatory argument, the size of the time bins over which the clicks are averaged to compute the intensity trace. Smaller bins provide a greater time resolution at the expense of less accuracy due to the stochastic nature of the emission and detection process. Additionally, one can specify which autocorrelator channel should be used to build the time trace if the user wants to separate the counts from the different channels. Options are available to limit the range of records. Finally, the computation of the time trace can be parallelized by specifying the number of threads to be used.

The computation of the second order autocorrelation is available via the *calculate_g2* function. In this case, the only mandatory argument is the length of the correlation window. The optional arguments allow the user to specify the time resolution of the histogram. The default value in this case is to split the histogram into 1024 bins if a time in seconds is not specified. The argument *post_selec_ranges* takes a list of pairs of values with start and stop records. Only clicks belonging to records within one of those ranges are used to compute $g^{(2)}$. As discussed above, this option allows users, for example, to exclude time ranges where they suspect photons likely only correspond to laser background. readPTU provides the function *construct_postselect_vector* to automatically generate ranges based on a hard threshold. The script used to analyze and produce the plots in figure 5 is available on the code repository together with instructions on how to extend the library to manipulate other file formats.

3 Example: resonance fluorescence of a quantum emitter with spectral fluctuations

One application of the functionalities offered by readPTU is to study the dynamics of single photon emitters. For solid-state emitters, fluctuations in the surrounding environment result in randoms shifts of the absorption/emission wavelength [17]. When exciting narrow absorption lines with

2019 JINST 14 T06011

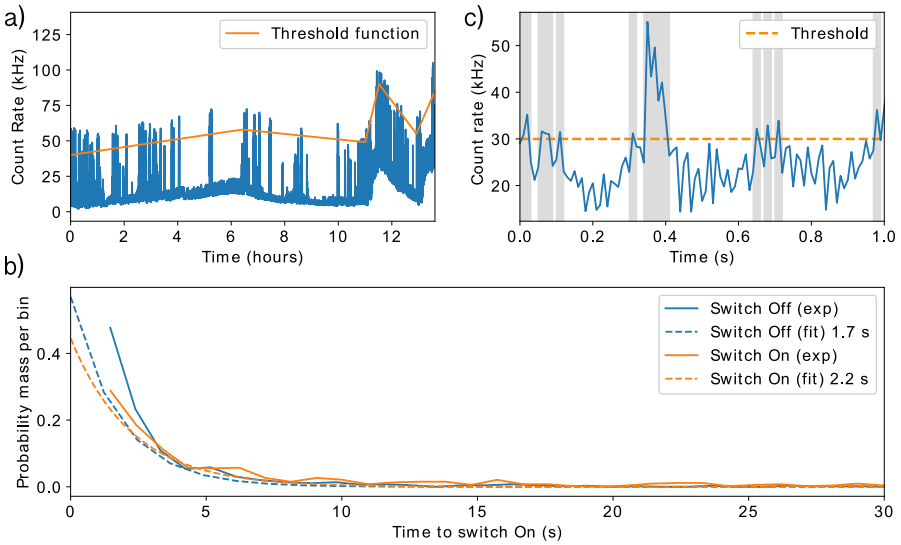

Figure 4. a) Intensity time trace of resonance fluorescence from a quantum dot in monolayer WSe_2. As the emitter wavelength jitters, it goes in and out of resonance randomly. When the emitter is out of resonance, only background laser photons are collected. By applying time post-selection, only photon count rates above a certain threshold are employed to compute the autocorrelation function. b) Zoom in of the intensity trace shown in a). Only photons collected during the highlighted windows of time are used to compute $g^{(2)}(\tau)$. c) Probability distribution for the duration of the time intervals during which the emitter is in the on/off state.

a narrowband lasers, these random shift bring the emitter in and out of resonance with the laser, resulting in intermittent optical emission [18, 19]. When the emitter is not resonant with the laser, only background light is collected, degrading the Signal to Background Ratio (SBR), an important parameter for antibunching experiments. In resonance fluorescence, the background laser can be filtered by polarization from the signal [20], but it remains challenging to completely remove it. This problem can be solved by post-selecting such that only the photons detected in time intervals when the emitter was resonant with the laser, i.e. when the emission rate is above a given threshold, contribute to the $g^{(2)}(\tau)$ measurement.

Here we show how readPTU can be used to analyze TCSPC data from a single photon emitter in an atomically-thin monolayer of WSe_2 [19], at cryogenic temperature. The emitters were addressed by resonance fluorescence in a confocal microscope. The laser linewidth is 10 kHz, while the emitter (typical linewidth $\approx$ 100 MHz) wavelength fluctuates on 10 GHz scale. While the timescales of the spectral fluctuations vary, they are relatively slow with dynamics longer than a second which can be easily post-selected for.

First, we extract an intensity timetrace. To this end, the user only has to specify the size of time bin over which the number of photons will be averaged, optionally the channel number. The timetrace helps us identify problems during the experiment, such as drifts of the experimental setup or blinking, as can be observed in figure 4. When the emitter goes out of resonance, the count number falls drastically to the level of the background produced by the uncancelled excitation laser. It can also be observed how the background laser cancellation fidelity drifts throughout the experiment. We use this information to design a piece-wise linear post-selection thresholding function adapted to our data.

2019 JINST 14 T06011

Once a threshold has been established, we can look at the distribution of the duration of periods for which the emitter has been in/out of resonance. This shows that the emitter was above threshold for just 0.5% of the duration of the experiment, due to the presence of charge traps that perturb the emitter's electrical environment. The dynamics of the short lived charge trap states are shown in figure 4. As expected the distribution of time intervals for which the emitter is in the on (off) state follow approximately an exponential distribution with a mean lifetime of 1.75 s (2.24 s).

Since only laser light is detected most of the time, the mininmum achieavable $g^2(0)$ is limited by the SBR averaged over the whole duration of the experiment, which is much smaller than the peak SBR. By post-selecting with the threshold function shown in figure 4, the minimum $g^2(0)$ is improved from 0.74 to 0.23 which demonstrates that the observed system is really a single emitter, since $g^{(2)} < 0.5$ [12].

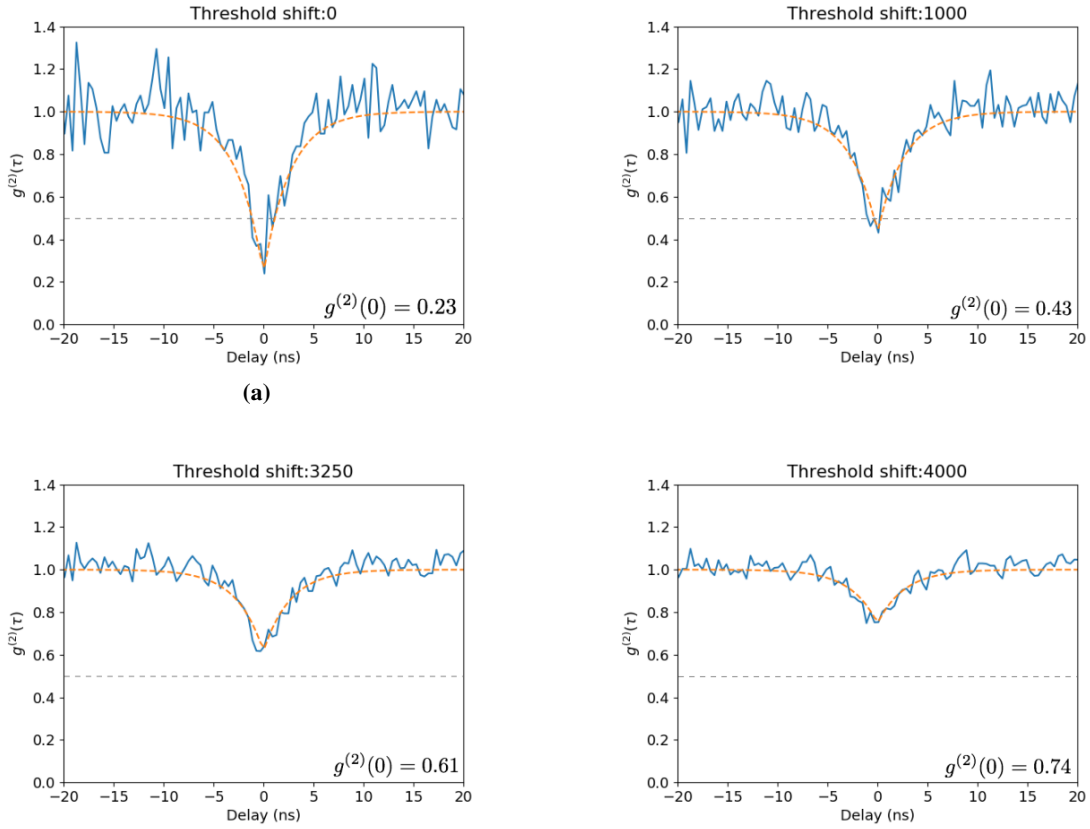

(a)

Figure 5. Second order autocorrelation as a function of the applied threshold. The legend on each plot shows the minimum $g^{(2)}(0)$ reached. The figure titles indicates the downwards shift in Hz that was applied to the optimum threshold function. As the threshold is lower more background photons are allowed into the second order autocorrelation computation decreasing the $g^{(2)}(0)$ value. When the threshold is shifted downwards by 4000 counts or more we obtain the same result regardless of the amount of postselection performed.

4 Conclusions

Here we present the implementation of multiple algorithms to compute the second order autocorrelation function from TCSPC data. Lifetime measurements can also be performed by choosing the appropiate parameters. The use of raw TCSPC data allows us to perform time post-selection of the data based on the intensity. This can be used to significantly improve experimental results in the resence of emitter blinking or spectral fluctuations [19]. Thanks to the focus on performance and extensibility multi-GB files can be analyzed in a few seconds and new algorithms can be implemented without having to worry about low levels details. More importantly, we have found that keeping raw TCSPC data has helped us improve our experimental setups and data analysis routines and having a library capable of efficiently analyzing it has promoted that it is always stored.

Acknowledgments

This work has been supported by the Engineering and Physical Sciences Research Council (EPSRC) under the grants: EP/I023186/1, EP/L015110/1, EP/S000550/1 and by the European Research Counil (ERC) under grant number 725920. B.D.G. thanks the Royal Society for a Wolfson Merit Award and the Royal Academy of Engineering for a Chair in Emergent Technologies.

References

[1] B. Lounis and W.E. Moerner, *Single photons on demand from a single molecule at room temperature*, *Nature* **407** (2000) 491.

[2] X. Ding et al., *On-demand single photons with high extraction efficiency and near-unity indistinguishability from a resonantly driven quantum dot in a micropillar*, *Phys. Rev. Lett.* **116** (2016) 020401.

[3] T. Niehörster et al., *Multi-target spectrally resolved fluorescence lifetime imaging microscopy*, *Nature Meth.* **13** (2016) 257.

[4] Q. Pian, R. Yao, N. Sinsuebphon and X. Intes, *Compressive hyperspectral time-resolved wide-field fluorescence lifetime imaging*, *Nature Photon.* **11** (2017) 411.

[5] J. Handsteiner et al., *Cosmic bell test: measurement settings from milky way stars*, *Phys. Rev. Lett.* **118** (2017) 060401 [arXiv:1611.06985].

[6] K. Suhling, P.M.W. French and D. Phillips, *Time-resolved fluorescence microscopy*, *Photochem. Photobiol. Sci.* **4** (2005) 13.

[7] A.C. Dada et al., *Indistinguishable single photons with flexible electronic triggering*, *Optica* **3** (2016) 493.

[8] A. Sipahigil et al., *Indistinguishable photons from separated silicon-vacancy centers in diamond*, *Phys. Rev. Lett.* **113** (2014) 113602.

[9] T.D. Ladd et al., *Quantum computers*, *Nature* **464** (2010) 45.

[10] W.B. Gao, P. Fallahi, E. Togan, J. Miguel-Sánchez and A. Imamoglu, *Observation of entanglement between a quantum dot spin and a single photon*, *Nature* **491** (2012) 426.

[11] E. Togan et al., *Quantum entanglement between an optical photon and a solid-state spin qubit*, *Nature* **466** (2010) 730.

2019 JINST 14 T06011

[12] M. Fox, *Quantum optics: an introduction*, vol. 15. Oxford University Press, Oxford, U.K. (2006).

[13] Z. Lin, *Extensible timetag analyzer*, https://timetag.github.io, (2018).

[14] T. Bischof, *Photon correlation*, https://github.com/tsbischof/photon_correlation, (2013).

[15] R.J. Glauber, *The quantum theory of optical coherence*, *Phys. Rev.* **130** (1963) 2529.

[16] R. Proux, *Indistinguishability of the photons emitted by a semiconductor quantum dot under continuous-wave resonant excitation*, thesis, École normale supérieure — ENS, Paris, France, November 2015.

[17] J. Houel et al., *Probing single-charge fluctuations at a GaAs/AlAs interface using laser spectroscopy on a nearby InGaAs quantum dot*, *Phys. Rev. Lett.* **108** (2012) 107401.

[18] T.S. Santana et al., *Generating indistinguishable photons from a quantum dot in a noisy environment*, *Phys. Rev.* **B 95** (2017) 201410.

[19] S. Kumar et al., *Resonant laser spectroscopy of localized excitons in monolayer WSe_2*, *Optica* **3** (2016) 882.

[20] A.V. Kuhlmann et al., *A dark-field microscope for background-free detection of resonance fluorescence from single semiconductor quantum dots operating in a set-and-forget mode*, *Rev. Sci. Instrum.* **84** (2013) 073905.

2019 JINST 14 T06011